

General-Acid-Catalyzed Reactions of Hypochlorous Acid and Acetyl Hypochlorite with Chlorite Ion

Zhongjiang Jia, Dale W. Margerum,* and Joseph S. Francisco

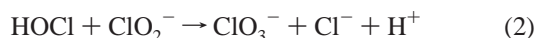
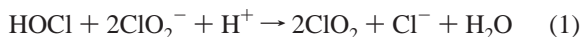
Department of Chemistry, Purdue University, West Lafayette, Indiana 47907

Received December 28, 1999

The rate of oxidation of ClO_2^- by HOCl is first order in each reactant and is general-acid catalyzed. In the initial steps of the proposed mechanism, a steady-state intermediate, HOClOClO^- , forms ($k_1 = 1.6 \text{ M}^{-1} \text{ s}^{-1}$) and undergoes general-acid (HA)-catalyzed reactions (k_2^{HA}) to generate a metastable intermediate, ClOClO . Values of k_2^{HA}/k_{-1} are $1.6 \times 10^4 \text{ M}^{-1} (\text{H}_3\text{O}^+)$, $20 \text{ M}^{-1} (\text{HOAc})$, and $8.5 \text{ M}^{-1} (\text{H}_2\text{PO}_4^-)$. Subsequent competitive reactions of ClOClO with ClO_2^- (k_3) to give 2ClO_2 and with OH^- (k_4^{OH}) and other bases (k_5^{B}) to give ClO_3^- are very rapid. The relative yields of these products give $k_4^{\text{OH}}/k_3 = 1.3 \times 10^5$, $k_5^{\text{HPO}_4}/k_3 = 0.20$, and $k_5^{\text{OAc}}/k_3 = 0.06$. At low pH and low buffer concentrations, the apparent yield of ClO_2 , based on 2ClO_2 per initial HOCl , reaches 140%. This anomaly is attributed to the induced disproportionation of ClO_2^- by ClOClO to give ClO_3^- and additional HOCl . A highly reactive intermediate, ClOCl(O)ClO^- , is proposed that can undergo Cl–O bond cleavage to give $2\text{ClO}_2 + \text{Cl}^-$ via one path and $\text{ClO}_3^- + 2\text{HOCl}$ via another path. The additional HOCl recycles in the presence of excess ClO_2^- to give more ClO_2 . Ab initio calculations show feasible structures for the proposed reaction intermediates. Acetic acid has a second catalytic role through the formation of acetyl hypochlorite, which is much more reactive than HOCl in the transfer of Cl^+ to ClO_2^- to form ClOClO .

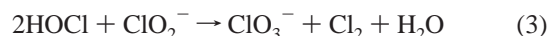
Introduction

Chlorine dioxide is used as an alternative to chlorine in water treatment^{1–3} and pulp bleaching⁴ because it is a strong oxidant and does not produce trihalomethanes and other organic halogens as does chlorine.⁵ In water treatment plants, chlorine dioxide is generated by mixing aqueous solutions of chlorine and sodium chlorite.^{1–3} Above pH 4, chlorine hydrolyzes to form hypochlorous acid. The reaction of HOCl with ClO_2^- forms ClO_2 (eq 1) and ClO_3^- (eq 2). The overall stoichiometry



of the reaction varies with the initial concentration ratio of the reactants and the pH. The yield of ClO_2 increases with increasing initial concentration of ClO_2^- and decreases with increasing pH.^{6–8} The USEPA has proposed a maximum contaminant level of 1.0 mg/L for chlorite ion^{9,10} and has suggested chlorate ion as a candidate for future regulation.¹¹

By using radioactive chlorine as a tracer, Taube and Dodgen¹² proposed an unsymmetrical intermediate, ClClO_2 (or ClOClO), which is common to the reactions in eqs 1 and 2. Imagawa, Fukagawa, and Yoshie¹³ reported that HOCl reacts with ClO_2^- to form ClO_2 ($d[\text{ClO}_2]/dt = k[\text{ClO}_2^-]^2[\text{HOCl}]$, $k = 3.2 \times 10^3 \text{ M}^{-2} \text{ s}^{-1}$). Subsequently, Peintler, Nagypál, and Epstein⁷ investigated this reaction in 0.5 M acetate buffer at pH 5–6 by monitoring the formation of ClO_2 . They found only a first-order dependence in $[\text{ClO}_2^-]$. In excess ClO_2^- , eq 1 was the stoichiometric reaction, and they reported the rate expression to be $d[\text{ClO}_2]/dt = 2k[\text{HOCl}][\text{H}^+][\text{ClO}_2^-]$, where $k = 1.1 \times 10^6 \text{ M}^{-2} \text{ s}^{-1}$. In excess HOCl , however, eq 3 was proposed to



explain the decrease in ClO_2 yield with increasing $[\text{HOCl}]_0$ because of ClO_3^- formation, where $-d[\text{ClO}_2^-]/dt = k[\text{HOCl}]^2[\text{ClO}_2^-]$, $k = 2.1 \times 10^3 \text{ M}^{-2} \text{ s}^{-1}$. (The abstract of that paper erroneously gave a value of $2.1 \times 10^{-3} \text{ M}^{-2} \text{ s}^{-1}$ for this rate constant.) Gordon and Tachiyashiki⁸ studied the $\text{HOCl}/\text{ClO}_2^-$ reaction in 0.1 M phosphate buffer at pH 6–10 and $[\text{OCl}^-]_0/[\text{ClO}_2^-]_0$ ratios of 0.5–2.0. The minor amount of ClO_2 that was produced gradually decreased over a period of 50 h. The formation of ClO_3^- was the dominant reaction, and the proposed

(1) Vigneswaran, S.; Vigneswaran, C. *Water Treatment Processes: Simple Options*; CRC Press: Boca Raton, FL, 1995; pp 191–208.

(2) Cheremisinoff, N. P.; Cheremisinoff, P. N. *Water Treatment and Waste Recovery: Advanced Technology and Applications*; PTR Prentice Hall: Englewood Cliffs, NJ, 1993; pp 64–68.

(3) Aieta, E. M.; Boyes, W.; Grasso, D.; Longley, K. E.; Robson, C. M.; Rogers, S. E.; Scheible, O. K.; Williams, R. E.; White, G. C.; Zeh, T. G. In *Wastewater Disinfection*; Chou, L., Sinozich, P., Eds.; Water Pollution Control Federation: Alexandria, VA, 1986; pp 65–69.

(4) Howard, W.; Strumila, G. B. In *The Bleaching of Pulp*, 3rd ed.; Singh, R. P., Ed.; Tappi Press: Atlanta, GA, 1979; pp 113–157.

(5) Werdehoff, K. S.; Singer, P. C. *J. AWWA* **1987**, *79*, 107–113.

(6) Tang, T. F.; Gordon, G. *Environ. Sci. Technol.* **1984**, *18*, 212–216.

(7) Peintler, G.; Nagypál, I.; Epstein, I. R. *J. Phys. Chem.* **1990**, *94*, 2954–2958.

(8) Gordon, G.; Tachiyashiki, S. *Environ. Sci. Technol.* **1991**, *25*, 468–474.

(9) USEPA. National Primary Drinking Water Regulations; Disinfectants and Disinfection Byproducts; Proposed Rule. *Fed. Regist.* **1994**, *59*, 38668–38829.

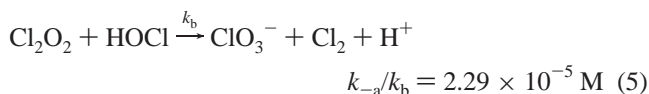
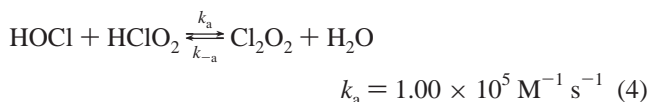
(10) USEPA. National Primary Drinking Water Regulations; Disinfectants and Disinfection Byproducts Notice of Data Availability; Proposed Rule. *Fed. Regist.* **1998**, *63*, 15674–15692.

(11) USEPA. Priority List of Substances Which May Require Regulation under the Safe Drinking Water Act. *Fed. Regist.* **1991**, *56*, 1470–1474.

(12) Taube, H.; Dodgen, H. *J. Am. Chem. Soc.* **1949**, *71*, 3330–3336.

(13) Imagawa, H.; Fukagawa, M.; Yoshie, T. *Nippon Kagaku Kaishi* **1974**, *2*, 238–243.

mechanism is shown in eqs 4 and 5, where Cl_2O_2 was treated as a steady-state species.



In the previous studies,^{7,8} the effect of buffer concentrations was ignored and the mechanism for eq 5 with Cl_2 formation was not clear. Furman and Margerum¹⁴ observed a strong buffer effect on the rates of the $\text{HOBr}/\text{ClO}_2^-$ reaction at pH 5–9. A mechanism was proposed for this reaction with HOBrOClO^- (or HOBrClO_2^-) as a steady-state species that undergoes general-acid-catalyzed reactions to form a highly reactive intermediate, BrOClO (or BrClO_2). The subsequent rapid reactions of BrOClO (or BrClO_2) with OH^- yield ClO_3^- , while competitive reactions with ClO_2^- lead to ClO_2 formation. From studies of the $\text{Cl}_2/\text{ClO}_2^-$ reaction in strong acidic solutions, Emmenegger and Gordon¹⁵ reported that greater than 100% yields of ClO_2 were obtained on the basis of the stoichiometry of eq 1. They suggested catalyzed disproportionation of ClO_2^- might take place, but no mechanism was given. In the present work, we show that phosphate and acetate buffers have large effects on the kinetics of the reaction between HOCl and ClO_2^- and the yield of ClO_2 . Mechanisms are proposed to explain the anomaly of greater than 100% yields of ClO_2 . The reactivities and mechanisms are compared for the $\text{HOCl}/\text{ClO}_2^-$ and the $\text{HOBr}/\text{ClO}_2^-$ reactions.

Experimental Section

Reagents. Doubly distilled, deionized water was used for solution preparations. "Chloride-free" hypochlorite solution was prepared by the reaction of yellow HgO with Cl_2 (99.9+%) in CCl_4 at 0 °C with stirring to form Cl_2O .¹⁶ The resulting Cl_2O solution was filtered, and the filtrate was extracted with ice-cooled NaOH solution to give "Cl⁻-free" NaOCl solution. The hypochlorite solution was standardized spectrophotometrically at 292 nm ($\epsilon_{\text{OCl}^-} = 362 \text{ M}^{-1} \text{ cm}^{-1}$).¹⁴ Sodium chlorite was recrystallized by literature procedures.^{7,14,17} The purity of the recrystallized NaClO_2 was determined to be 98.7% by iodometric titrimetry. Dilute solutions of ClO_2^- were standardized spectrophotometrically at 260 nm ($\epsilon = 154 \text{ M}^{-1} \text{ cm}^{-1}$).¹⁴ Solution ionic strength (μ) was adjusted with NaClO_4 that was recrystallized from water. All studies were carried out at 25.0 °C and $\mu = 1.0 \text{ M}$.

Instrumental Methods. The measured pH was corrected to $\text{p}[\text{H}^+]$ at 25.0 ± 0.1 °C and $\mu = 1.0 \text{ M}$.¹⁴ Kinetic studies were performed on an Applied PhotoPhysics SX.18MV stopped-flow spectrophotometer (APPSF, optical path length = 0.962 cm). The progress of the $\text{HOCl}/\text{ClO}_2^-$ reactions was followed by observing the formation of ClO_2 at 360 nm ($\epsilon_{\text{ClO}_2} = 1230 \text{ M}^{-1} \text{ cm}^{-1}$)¹⁴ under pseudo-first-order conditions with ClO_2^- in large excess over HOCl . All rate constants are an average of three to five runs. Gordon and Emmenegger¹⁸ reported that ClO_2 and ClO_2^- can form a complex with a formation constant of 1.6 M^{-1} and molar absorptivity of $900 \text{ M}^{-1} \text{ cm}^{-1}$ at 360 nm. However, the absorbance of ClO_2^- at 360 nm was not taken into account in their

measurements, and we find no evidence of appreciable $\text{ClO}_2-\text{ClO}_2^-$ complex formation. Detailed experimental procedures for the determination of ClO_3^- by capillary electrophoresis were described in the previous paper.¹⁴

Results and Discussion

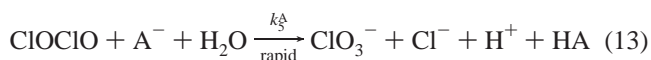
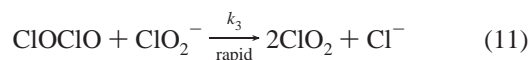
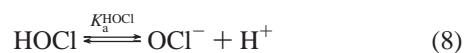
Kinetics and ClO_2 Yield. The rate expression is defined in eq 6, where $[\text{HOCl}]_T = [\text{HOCl}] + [\text{OCl}^-]$. In terms of the formation of ClO_2 , the integrated rate expression is given in eq 7. The yield of ClO_2 is calculated on the basis of the limiting

$$-\frac{d[\text{HOCl}]_T}{dt} = k_{\text{obsd}}[\text{HOCl}]_T \quad (6)$$

$$\ln\left(\frac{[\text{ClO}_2]_{\infty}}{[\text{ClO}_2]_{\infty} - [\text{ClO}_2]_t}\right) = k_{\text{obsd}}t \quad (7)$$

reagent $[\text{HOCl}]_T$ and the stoichiometry in eq 1. The observed first-order rate constants (k_{obsd}) vary with $[\text{ClO}_2^-]$, $[\text{H}^+]$, and $[\text{buffer}]_T$. In phosphate buffer, the k_{obsd} values have a first-order dependence on $[\text{ClO}_2^-]$, while the yields of ClO_2 increase with $[\text{ClO}_2^-]$ and approach 100% (Figure 1). Therefore, the observed first-order rate constants do not depend on the yield of ClO_2 , which indicates that the formation of ClO_2 and ClO_3^- occurs after the rate-determining steps. A mechanism is needed in which an intermediate is formed from the interaction of HOCl , ClO_2^- , and general acids in the rate-determining steps. This intermediate must react very rapidly either with another ClO_2^- to give 2ClO_2 or with OH^- to give ClO_3^- . The proposed mechanisms are based both on detailed kinetic data that define the rate-determining steps and on the yields of products which depend on competitive reactions after the rate-determining steps.

Proposed Mechanism for the $\text{HOCl}/\text{ClO}_2^-$ Reaction (General-Acid Path). A mechanism in eqs 8–13 is proposed for the $\text{HOCl}/\text{ClO}_2^-$ reaction that is similar to the $\text{HOBr}/\text{ClO}_2^-$



reaction.¹⁴ A steady-state species, HOClOClO^- , is formed (eq 9) which undergoes general-acid-catalyzed reactions to form ClOClO (eq 10). Scheme 1 illustrates the proposed general-acid-catalyzed path to form ClOClO . In subsequent rapid reactions, ClOClO reacts with ClO_2^- to form ClO_2 (eq 11) and reacts with OH^- and H_2O , assisted by a general base (A^-), to form ClO_3^- (eqs 12 and 13) as shown in Scheme 2.

The $\text{p}K_a$ value of HClO_2 is 1.72 at 25.0 °C and $\mu = 1.0 \text{ M}$.¹⁷ At pH 4.7–7.5, almost all Cl(III) is in the form of ClO_2^- . The

(14) Furman, C. S.; Margerum, D. W. *Inorg. Chem.* **1998**, *37*, 4321–4327.

(15) Emmenegger, F.; Gordon, G. *Inorg. Chem.* **1967**, *6*, 633–635.

(16) (a) Johnson, D. W.; Margerum, D. W. *Inorg. Chem.* **1991**, *30*, 4845–4851. (b) Cady, G. H. *Inorg. Synth.* **1957**, *5*, 156–165.

(17) Fabian, I.; Gordon, G. *Inorg. Chem.* **1991**, *30*, 3785–3787.

(18) Gordon, G.; Emmenegger, F. *Inorg. Nucl. Chem. Lett.* **1966**, *2*, 395–398.

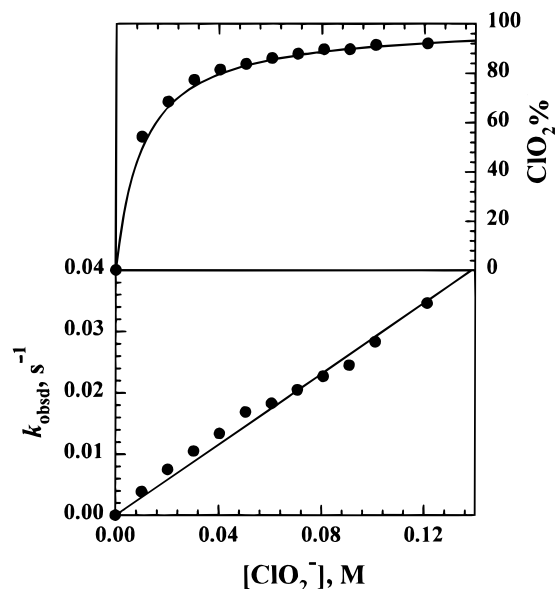
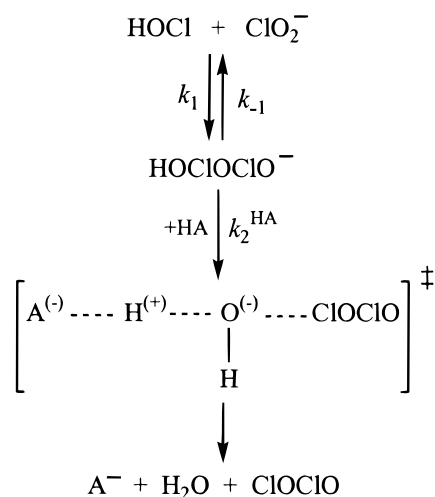


Figure 1. Dependence of observed first-order rate constants (k_{obsd}) and ClO_2 yields on $[\text{ClO}_2^-]$ in phosphate buffer. Conditions: $[\text{HOCl}]_{\text{T}} = 7.17 \times 10^{-5} \text{ M}$, $\text{p}[\text{H}^+] = 6.44 \pm 0.01$, $[\text{PO}_4]_{\text{T}} = 0.10 \text{ M}$, $25.0 \text{ }^\circ\text{C}$, $\mu = 1.0 \text{ M}$.

Scheme 1. General-Acid (HA)-Assisted Path To Form ClOClO



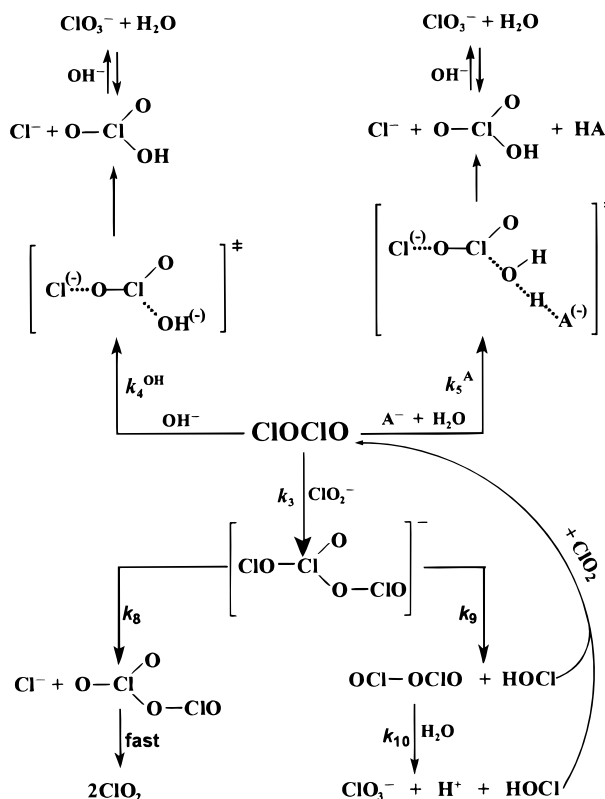
rate expressions (eqs 14 and 15) are derived from the above

$$-\frac{d[\text{HOCl}]_{\text{T}}}{dt} = \frac{k_1 \left(\sum \frac{k_2^{\text{HA}}}{k_{-1}} [\text{HA}] \right) [\text{ClO}_2^-] [\text{HOCl}]_{\text{T}} \left[\frac{[\text{H}^+]}{[\text{H}^+] + K_a^{\text{HOCl}}} \right]}{1 + \sum \frac{k_2^{\text{HA}}}{k_{-1}} [\text{HA}]} \quad (14)$$

$$k_{\text{obsd}} = \frac{k_1 \left(\sum \frac{k_2^{\text{HA}}}{k_{-1}} [\text{HA}] \right) [\text{ClO}_2^-] \left[\frac{[\text{H}^+]}{[\text{H}^+] + K_a^{\text{HOCl}}} \right]}{1 + \sum \frac{k_2^{\text{HA}}}{k_{-1}} [\text{HA}]} \quad (15)$$

mechanism, in which HA is the general acid (H_3O^+ , H_2PO_4^- , HOAc , or H_2O). The $\text{p}K_a^{\text{HOCl}}$ value of 7.47 ($25.0 \text{ }^\circ\text{C}$, $\mu = 1.0$

Scheme 2. Pathways for the Formation of ClO_2 and ClO_3^- from ClOClO



M)¹⁹ is used to correct for OCl^- at high pH because it is not a reactive species.

The yield of ClO_2 (eq 16) depends on the competition among the reactions of ClOClO with ClO_2^- (eq 11), OH^- (eq 12), and H_2O (eq 13). The reactions in eqs 11–13 only affect the yield

$$\% \text{ClO}_2 = \frac{2k_3[\text{ClO}_2^-]}{k_5^{\text{A}}[\text{A}^-] + k_4^{\text{OH}}[\text{OH}^-] + 2k_3[\text{ClO}_2^-]} \times 100 \quad (16)$$

of ClO_2 , not the rate. The yield of ClO_2 increases with increasing $[\text{ClO}_2^-]$ (Figure 1) and decreases with increasing phosphate buffer concentration (Figure 2) and with increasing pH (Figure 3). Curve-fitting the yields of ClO_2 to eq 16 gives $k_4^{\text{OH}}/k_3 = (1.3 \pm 0.1) \times 10^5$ and $k_5^{\text{H}_2\text{PO}_4^-}/k_3 = 0.20 \pm 0.02$.

p[H⁺] and Phosphate Buffer Dependence on k_{obsd} . The observed first-order rate constants increase with decreasing $\text{p}[\text{H}^+]$ (Figure 3). This is because acid converts OCl^- to the reactive form of HOCl (eq 8) and also reacts with the intermediate, HOCIOClO^- , to form ClOClO and H_2O (eq 10). In addition, our results show that the observed first-order rate constants increase with increasing $[\text{H}_2\text{PO}_4^-]$ (Figure 2). General acids such as H_2PO_4^- can assist the reaction by transferring a proton to HOCIOClO^- to form ClOClO and H_2O (eq 10). The buffer effect has been ignored in the previous studies.^{7,8} Least-squares fitting of the observed rate constants with $[\text{H}^+]$ and $[\text{H}_2\text{PO}_4^-]$ to eq 15 gives $k_1 = 1.6 \pm 0.1 \text{ M}^{-1} \text{ s}^{-1}$, $k_2^{\text{H}_2\text{PO}_4^-}/k_{-1} = 8.5 \pm 0.9 \text{ M}^{-1}$, and $k_2^{\text{H}}/k_{-1} = (1 \pm 1) \times 10^4 \text{ M}^{-1}$. A more accurate value of k_2^{H}/k_{-1} is obtained from the studies in acetate buffer. The value of $k_2^{\text{H}_2\text{O}}/k_{-1}$ is negligible.

HOCl/ ClO_2^- Reactions in Acetate Buffer. A strong acetate buffer dependence for the k_{obsd} values was observed as shown

(19) Gerritsen, C. M.; Margerum, D. W. *Inorg. Chem.* **1990**, *29*, 2757–2762.

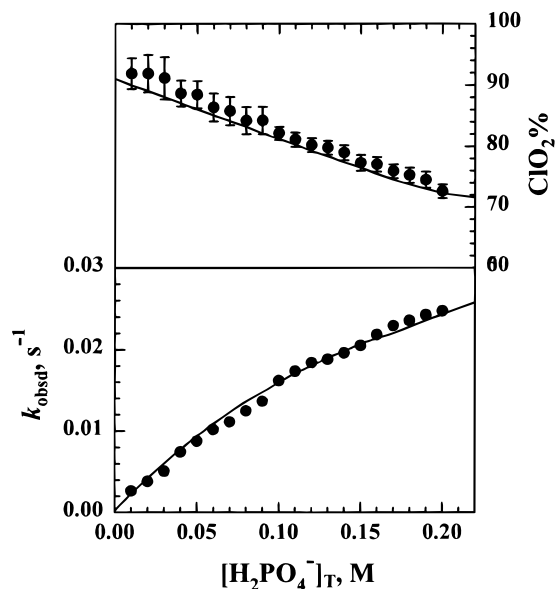


Figure 2. Phosphate buffer effect on the rate constants and yields of ClO_2 . Conditions: $[\text{ClO}_2^-] = 0.0444 \text{ M}$, $[\text{HOCl}]_{\text{T}} = 1.11 \times 10^{-4} \text{ M}$, $\text{p}[\text{H}^+] = 6.45 \pm 0.02$, $25.0 \text{ }^\circ\text{C}$, $\mu = 1.0 \text{ M}$.

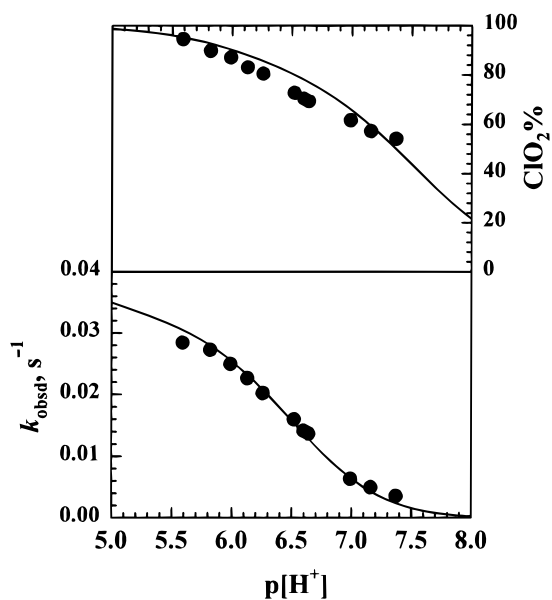


Figure 3. Effect of $\text{p}[\text{H}^+]$ on the observed first-order rate constants (k_{obsd}) and yields of ClO_2 in phosphate buffer. Conditions: $[\text{ClO}_2^-] = 0.0475 \text{ M}$, $[\text{HOCl}]_{\text{T}} = 1.01 \times 10^{-4} \text{ M}$, $[\text{PO}_4]_{\text{T}} = 0.10 \text{ M}$, $25.0 \text{ }^\circ\text{C}$, $\mu = 1.0 \text{ M}$.

in Figure 4. From the intercept of Figure 4 and the k_1 value determined in the phosphate buffer studies, the value of k_2^{H}/k_{-1} is calculated to be $(1.6 \pm 0.5) \times 10^4 \text{ M}^{-1}$, in accord with eq 15. The value of $k_2^{\text{H}_2\text{O}}/k_{-1}$ is negligible. The yields of ClO_2 , which appear to be greater than 140% at low acetate concentrations, decrease to 102% with increasing total acetate buffer concentration (from 0.02 to 0.6 M) at $\text{p}[\text{H}^+] 4.70$ (Figure 4). The anomalously high ClO_2 yields are not due to $[\text{HOAc}]_{\text{T}}$. Indeed, we propose the ClO_2 yields decrease in Figure 4 because OAc^- assists the hydrolysis of ClOClO to form ClO_3^- and Cl^- (eq 13). Figure 5 shows that the rate of the $\text{HOCl}/\text{ClO}_2^-$ reaction in acetate buffer does not have a simple first-order dependence on $[\text{ClO}_2^-]$. The yield of ClO_2 first increases (to a maximum of 116%) and then decreases to 101% as $[\text{ClO}_2^-]$ increases. Two aspects of the behavior of these $\text{HOCl}/\text{ClO}_2^-$ reactions need to be addressed. We will first consider why the observed

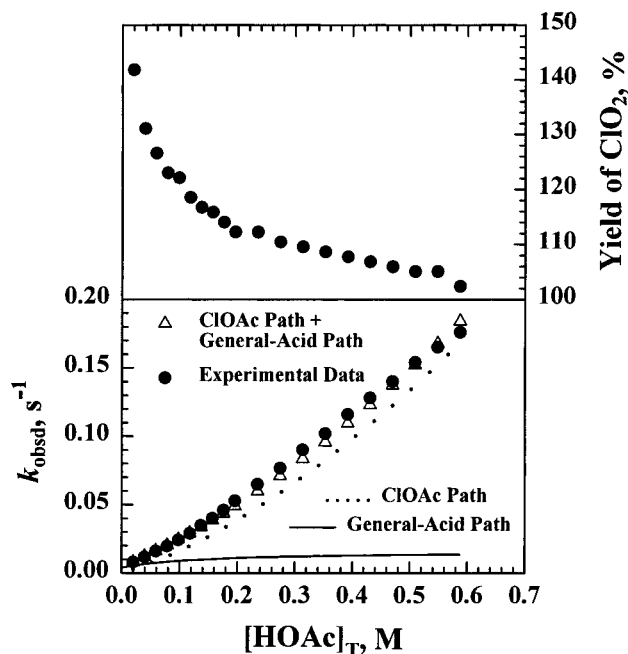


Figure 4. Acetate buffer effect on the rate constants and ClO_2 yields. Conditions: $[\text{ClO}_2^-] = 0.0101 \text{ M}$, $[\text{HOCl}]_{\text{initial}} = 4.71 \times 10^{-5} \text{ M}$, $\text{p}[\text{H}^+] = 4.70 \pm 0.01$, $25.0 \text{ }^\circ\text{C}$, $\mu = 1.0 \text{ M}$.

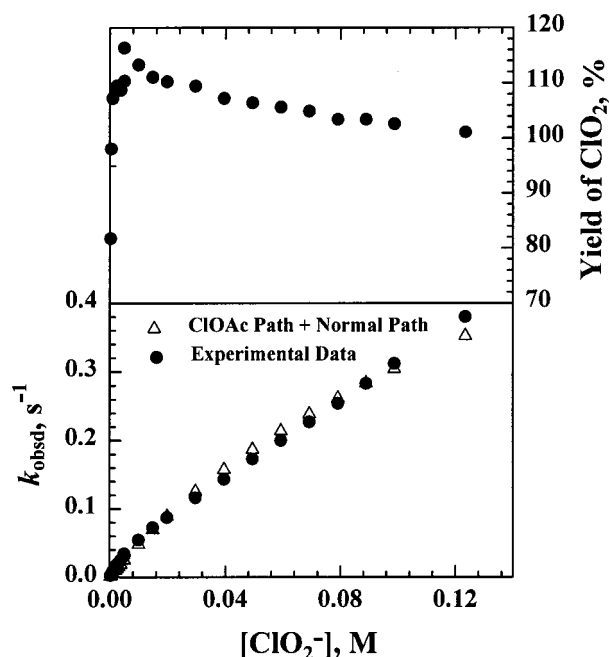
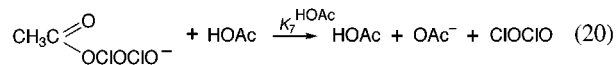
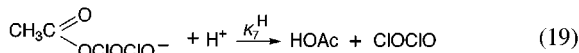
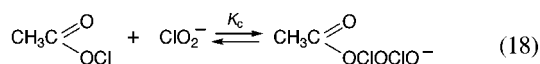
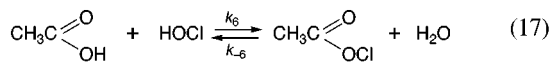


Figure 5. Dependence of the rate constants and the yields of ClO_2 on $[\text{ClO}_2^-]$ in acetate buffer. Conditions: $[\text{HOCl}]_{\text{initial}} = 5.56 \times 10^{-5} \text{ M}$, $\text{p}[\text{H}^+] = 4.71 \pm 0.01$, $[\text{HOAc}]_{\text{T}} = 0.2034 \text{ M}$, $25.0 \text{ }^\circ\text{C}$, $\mu = 1.0 \text{ M}$.

first-order rate constants in high concentrations of acetate buffer are much greater than expected from the general-acid path (eqs 8–13). The extent of this deviation is shown in Figure 4. Then we will discuss reasons that the apparent yields of ClO_2 at low pH can become much larger than 100%.

Proposed Acetyl Hypochlorite Mechanism for the $\text{HOCl}/\text{ClO}_2^-$ Reaction in Acetate Buffer. Acetyl hypochlorite, $\text{CH}_3\text{C}(\text{O})\text{OCl}$ (or ClOAc), has been prepared by the reaction of Cl_2 with mercuric or silver acetate in glacial acetic acid.²⁰ Rate constants of $0.1\text{--}0.24 \text{ M}^{-1} \text{ s}^{-1}$ have been reported for the

reaction of HOCl and HOAc to form ClOAc.^{21–23} An acetyl hypochlorite path (eqs 17–20) is proposed for the HOCl/ClO₂[−]



reaction in acetate buffer in addition to the general-acid path (eqs 8–13). Acetyl hypochlorite is formed from HOCl and HOAc (eq 17), and it reacts rapidly with ClO₂[−] to form an adduct, AcOClOClO[−] (eq 18). This adduct can undergo general-acid-catalyzed reactions to form ClOClO (eqs 19 and 20), which reacts rapidly with ClO₂[−], OH[−], and OAc[−] (eqs 11–13). Equation 18 is proposed as a rapid equilibrium unlike eq 9 because ClOAc is a better electrophile than HOCl.²⁴ The equilibrium formation constant of ClOAc (measured in acetic acid with low H₂O concentrations) is only 0.0025.²⁵ Therefore, acetyl hypochlorite and its ClO₂[−] adduct are treated as combined steady-state species. The observed first-order rate constant is derived in eq 21.

$$k_{\text{obsd}} = \frac{k_6 K_C [\text{HOAc}] [\text{ClO}_2^-] (k_7^{\text{H}} [\text{H}^+] + k_7^{\text{HOAc}} [\text{HOAc}])}{k_{-6} + K_C (k_7^{\text{H}} [\text{H}^+] + k_7^{\text{HOAc}} [\text{HOAc}]) [\text{ClO}_2^-]} \quad (21)$$

In the proposed mechanism (eqs 17–20), HOAc has two roles. One is to form a very strong Cl⁺-transfer agent (eq 17), and the other is to assist the breakup of the AcOClOClO[−] adduct (eq 20). This gives a much larger acceleration to the rate than the “normal” role of HOAc as a general acid (eq 10). The kinetic data from acetate buffer dependence (Figure 4) and [ClO₂[−]] dependence (Figure 5) are fit to the sum of eq 15 for the general-acid path and eq 21 for the ClOAc path. Figure 4 shows the domination of the ClOAc path compared to the general-acid path. Previous estimates^{21–23} of the *k*₆ value have not considered the importance of a much larger *k*_{−6} value (i.e., reversibility). Our steady-state treatment gives a *k*₆ value of 4.5 M^{−1} s^{−1}, which is 20 times larger than the previous estimates. The resolved rate constants are summarized in Table 1.

The Brønsted–Pedersen relationship²⁶ for the *k*₂^{HA}/*k*_{−1} term (eq 22) gives log *G*_a = 3.14 ± 0.04 and α = 0.41 ± 0.01, where the p*K*_a^{HA} values are −1.72 (H₃O⁺), 4.61 (HOAc),²⁷ and

$$\log \left(\frac{k_2^{\text{HA}}}{k_{-1} p} \right) = \log G_a + \alpha \log \left(\frac{K_a^{\text{HA}} q}{p} \right) \quad (22)$$

6.26 (H₂PO₄[−]);¹⁴ *p* is the number of equivalent protons on HA,

(21) Israel, C. C. *J. Chem. Soc.* **1950**, 1286–1289.

(22) Chung, A.; Israel, C. C. *J. Chem. Soc.* **1955**, 2667–2673.

(23) Anbar, M.; Dostrovsky, I. *J. Chem. Soc.* **1954**, 1094–1104.

(24) de la Mare, P. B. D.; Hilton, I. C.; Varma, S. *J. Chem. Soc.* **1960**, 4044–4054.

(25) de la Mare, P. B. D.; Hilton, I. C.; Vernon, C. A. *J. Chem. Soc.* **1960**, 4039–4044.

(26) Bell, R. P. *The Proton in Chemistry*, 2nd ed.; Cornell University: Ithaca, NY, 1973; p 198.

(27) Portanova, R.; Bernardo, P. D.; Cassol, A.; Tondello, E.; Magon, L. *Inorg. Chim. Acta* **1974**, 8, 233–240.

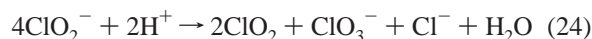
Table 1. Rate Constants for the Reactions of ClO₂[−] with HOCl and HOBr at μ = 1.0 M and 25.0 °C^a

rate const	HOBr/ClO ₂ [−] ^b	HOCl/ClO ₂ [−] ^c
<i>k</i> ₁ , M ^{−1} s ^{−1}	97 ± 6	1.6 ± 0.1
<i>k</i> ₂ ^H / <i>k</i> _{−1} , M ^{−1}	(3.1 ± 0.5) × 10 ⁵	(1.6 ± 0.5) × 10 ⁴
<i>k</i> ₂ ^{HOAc} / <i>k</i> _{−1} , M ^{−1}		20
<i>k</i> ₂ ^{H₂PO₄} / <i>k</i> _{−1} , M ^{−1}	8.3 ± 0.6	8.5 ± 0.9
<i>k</i> ₄ ^{OH} / <i>k</i> ₃	(6.83 ± 0.05) × 10 ³	(1.3 ± 0.1) × 10 ⁵
<i>k</i> ₅ ^{HPO₄} / <i>k</i> ₃		0.20 ± 0.02
<i>k</i> ₅ ^{OAc} / <i>k</i> ₃		0.06
<i>k</i> ₆ , M ^{−1} s ^{−1}		4.5 ± 0.3
<i>k</i> ₇ ^H <i>K</i> _C / <i>k</i> _{−6} , M ^{−2}		(2.8 ± 0.6) × 10 ⁵
<i>k</i> ₇ ^{HOAc} <i>K</i> _C / <i>k</i> _{−6} , M ^{−2}		46 ± 4
<i>k</i> ₉ / <i>k</i> ₈ , M ^{−1}		1 × 10 ⁴

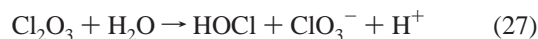
^a p*K*_a = 7.47 for HOCl, 6.26 for H₂PO₄[−], 4.61 for HOAc; p*K*_w = 13.60. ^b Reference 14. ^c This work.

and *q* is the number of equivalent basic sites on A[−]. The slope (α) of 0.41 indicates a significant degree of proton transfer from the general acid (HA) to HOClOClO[−] (Scheme 1) in the transition state. The value of *k*₂^{HOAc}/*k*_{−1} in the general-acid path is obtained from the fit of data to eqs 15 and 21 at low concentrations of acetate buffer. This value (20 M^{−1}) agrees with that estimated from the Brønsted–Pedersen relationship.

Greater Than 100% Yields of ClO₂ and ClOClO-Induced Disproportionation of ClO₂[−]. If eq 1 gives a 100% yield of ClO₂, then ClO₃[−] formation (eq 2) would not be expected because these two reactions are in competition with one another. However, our experimental results (Table 2) show that significant amounts of ClO₃[−] are generated even when yields of ClO₂ are greater than 100% (based on the initial limiting [HOCl]_T). The sums of the yields of ClO₂ and ClO₃[−] average 115% from pH 6.2 to 4.7. Since ClO₂[−] is in excess in these experiments, any disproportionation (eq 23) to give additional HOCl and



ClO₃[−] would account for this behavior, because the HOCl and ClO₂[−] would react further to give ClO₂ (eq 1) with the overall stoichiometry in eq 24. However, the rate of uncatalyzed ClO₂[−] disproportionation^{28–30} is much too slow to explain the observed effect. Hence, we propose the mechanism in eqs 25–27 to



account for a ClOClO-induced reaction that causes HOCl to be generated and thus leads to more ClO₂ than expected. The first step (eq 25) has the same reactants shown in eq 11, but we now suggest ClOCl(O)OCIO[−] as another intermediate that can dissociate via Cl–O bond cleavage to give different products. In one path (*k*₈ in Scheme 2), loss of a terminal Cl[−] leads to OCl(O)OCIO, an unstable dimer of ClO₂ that undergoes rapid homolytic bond cleavage to give 2ClO₂. In the other path (*k*₉ in Scheme 2), loss of ClO[−] from ClOCl(O)OCIO[−] generates HOCl and Cl₂O₃ (eq 26). The latter species can react with H₂O to give another HOCl and ClO₃[−] (eq 27). This second path provides additional HOCl that ultimately leads to higher yields

(28) Hong, C. C.; Rapson, W. H. *Can. J. Chem.* **1968**, 46, 2053–2060.

(29) Kieffer, R. G.; Gordon, G. *Inorg. Chem.* **1968**, 7, 235–239.

(30) Kieffer, R. G.; Gordon, G. *Inorg. Chem.* **1968**, 7, 239–244.

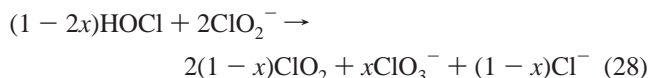
Table 2. Determination of ClO_3^- by CZE from the $\text{HOCl}/\text{ClO}_2^-$ Reaction in 0.02 M $[\text{HOAc}]_{\text{T}}^a$

p[H ⁺]	[HOCl] _T , mM	% ClO ₂	% ClO ₃ ⁻	Σ(% ClO ₂ + % ClO ₃ ⁻)
6.22	3.01	90	16 ± 1	106
5.42	1.50	105	11 ± 2	116
5.26	1.50	101	7.6 ± 0.4	109
5.19	3.01	96	8 ± 2	104
5.15	1.177	102	13 ± 2	115
5.05	1.05	109	6 ± 2	115
4.98	0.525	121	6 ± 1	127
4.72	1.177	106	19 ± 2	125

^a $[\text{ClO}_2^-] = 0.01$ M; pressure injection 25 mbar, 10 s; separation voltage -25 kV.

of ClO_2 even though ClO_3^- is also formed. Scheme 2 shows the proposed pathways to account for the effects of pH and buffer on the observed yields. It must be emphasized that these steps all occur after the rate-determining steps and are based on logical explanations of how the yields are affected by changes in conditions. The k_4^{OH} path accounts for the decreased yield of ClO_2 as the pH increases, and the k_5^{A} path explains why high acetate ion concentrations reduce the yield of ClO_2 .

At low pH and low buffer concentrations, the k_4^{OH} and k_5^{A} pathways are negligible. If the fraction of the $\text{ClOClO}/\text{ClO}_2^-$ reaction by the k_9 path is x , then the fraction of this reaction by k_8 path is $(1 - x)$. The overall stoichiometry is described in eq 28. The yields of ClO_2 and ClO_3^- in terms of HOCl are given in eqs 29 and 30. When $x = 0.2$, the predicted yield of ClO_2 is

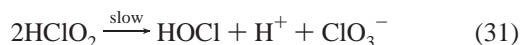


$$\% \text{ClO}_2 = \frac{1 - x}{1 - 2x} \times 100 \quad (29)$$

$$\% \text{ClO}_3^- = \frac{x}{1 - 2x} \times 100 \quad (30)$$

133%, which is close to the experimental result of 142% at pH 4.7 and $[\text{HOAc}]_{\text{T}} = 0.02$ M in Figure 4. As the $[\text{HOAc}]_{\text{T}}$ is increased to 0.5 M (Figure 4), the yield of ClO_2 drops to 105%. We suggest that the high OAc^- concentration causes this 37% decrease in ClO_2 yield, which would mean an 18.5% increase in ClO_3^- formation. This would correspond (approximately) to $k_5^{\text{OAc}}/k_3 = (0.185/0.105)([\text{ClO}_2^-]/[\text{OAc}^-]) = 0.06$, which is reasonable compared to values of $k_4^{\text{OH}}/k_3 = 1.3 \times 10^5$ and $k_5^{\text{HPO}_4}/k_3 = 0.20$, because OAc^- is a much weaker base. Much higher concentrations of HOCl were used in the CZE experiments. The ClO_2 and ClO_3^- yields in Table 2 at low pH correspond roughly to $x = 0.1$ (113% ClO_2 and 13% ClO_3^-).

Greater than 100% yields of ClO_2 were also observed in the $\text{Cl}_2/\text{ClO}_2^-$ reaction ($[\text{H}^+] = 0.2$ M)¹⁵ and in the disproportionation³¹ of ClO_2^- ($[\text{H}^+] = 0.01$ –2 M). The disproportionation of chlorous acid in the absence of Cl^- followed the same stoichiometry as in eq 24, where the limiting step was proposed to be the slow formation of HOCl (eq 31).^{28–30} We propose



that HOCl or Cl_2 will react with ClO_2^- to form ClOClO (eqs 9 and 10), which again reacts with ClO_2^- to form an adduct, ClOCl(O)ClO^- . At low pH, this adduct can generate more HOCl , which leads to more ClO_2 and ClO_3^- (Scheme 2). Our

(31) Schmitz, G.; Rooze, H. *Can. J. Chem.* **1981**, *59*, 1177–1187.

results disagree with the previous explanation⁸ for the formation of ClO_3^- from the reaction of Cl_2O_2 with HOCl (eq 5).

Structures of the Proposed Intermediates. To help understand if the proposed intermediates in Schemes 1 and 2 are plausible, ab initio calculations were used.^{32,33} Equilibrium geometries were determined from both B3LYP/6-31G* and B3YLP/6-311++G(3df, 3pd) calculations. The latter results give the molecular structures of the intermediates, bond distances, and atomic charges shown in Figure 6. One proposed intermediate, Cl_2O_3 , has been observed in the gas phase,³⁴ and ClOCl(O)O was calculated to be the most stable structure by Clark and Francisco.³³ The relative energetics of the reaction pathways are given in the Supporting Information. Aqueous solvation will undoubtedly have a large effect on their relative stabilities and reactivities. However, the calculated structures serve as useful models for the proposed intermediates.

Comparison between the $\text{HOCl}/\text{ClO}_2^-$ and $\text{HOBr}/\text{ClO}_2^-$ Reactions. Previous studies¹⁴ showed that HOBr and ClO_2^- react by the same mechanism as given in Scheme 1 for the HOCl and ClO_2^- reaction. The HOBr reactions are faster, where the k_1 step is a factor of 60 times larger than that for HOCl . The experimentally observed rate constants with acid-assisted contributions from H_3O^+ and H_2PO_4^- vary from 60 to 10^3 for $k_{\text{obsd}}^{\text{HOBr}}/k_{\text{obsd}}^{\text{HOCl}}$, depending on the pH and buffer concentrations.

There are several reasons why we prefer to designate the initial steady-state intermediates as chainlike structures, i.e., HOBrOClO^- and HOClOClO^- rather than Y-shaped structures with halogen–halogen bonds, i.e., HOBrCl(O)O^- and HOClCl(O)O^- . First, studies by Perrone and Margerum³⁵ of HOCl reactions with BrO_2^- require a chainlike adduct (HOClOBrO^-) to account for the formation of ClO_2 as a product. Second, ab initio calculations show the chainlike structure is preferred.³⁶ Third, the proposed mechanism in Scheme 2 with Cl_2O_3 as an intermediate is more favorable for ClOCl(O)O than for ClClO_3 .³³ We cannot rule out the possibility of some competing paths with halogen–halogen bonding for the intermediates, but we suggest that the chainlike structures are preferred.

Although the k_1 step corresponds to the formation of an adduct between a Lewis base (OClO^-) and a weak Lewis acid (HOCl or HOBr), the rate constants of 1.6 and $97 \text{ M}^{-1} \text{ s}^{-1}$ are much smaller than those for most Lewis acid–base reactions. Once again, ab initio calculations are helpful in understanding why this is the case. The O–Cl (1.707 Å) bond length in HOCl increases by 0.14 Å, and the O–Cl (1.576 Å) bond lengths in

- (32) Molecular orbital calculations were performed using the Gaussian 94 program: Frisch, M. J.; Trucks, G. W.; Schlegel, H. B.; Gill, P. M. W.; Johnson, B. G.; Robb, M. A.; Cheeseman, J. R.; Keith, T.; Petersson, G. A.; Montgomery, J. A.; Raghavachari, K.; Al-Laham, M. A.; Zakrzewski, V. G.; Ortiz, J. V.; Foresman, J. B.; Cioslowski, J.; Stefanov, B. B.; Nanayakara, A.; Challacombe, M.; Peng, C. Y.; Ayala, P. Y.; Chen, W.; Wong, M. W.; Andres, J. L.; Replogle, E. S.; Gomperts, R.; Martin, R. L.; Fox, D. J.; Binkley, J. S.; Defrees, D. J.; Baker, J.; Stewart, J. P.; Head-Gordon, M.; Gonzales, C.; Pople, J. A. *Gaussian 94*, Revision D.2; Gaussian, Inc.: Pittsburgh, PA, 1995.
- (33) All equilibrium geometrical parameters were fully optimized, using Schlegel's method, to better than 0.001 Å for bond distances and 0.10° for bond angles with a self-consistent field convergence of at least 10^{-9} on the density matrix: Clark, J.; Francisco, J. S. *J. Phys. Chem. A* **1997**, *101*, 7145–7153.
- (34) (a) Hayman, G. D.; Cox, R. A. *Chem. Phys. Lett.* **1989**, *155*, 1–7. (b) Burkholder, J. B.; Mauldin, R. L., III; Yokelson, R. J.; Solomon, S.; Ravishankara, A. R. *J. Phys. Chem.* **1993**, *97*, 7597–7605. (c) Friedl, R. R.; Birk, M.; Oh, J. J.; Cohen, E. A. *J. Mol. Spectrosc.* **1995**, *170*, 383–396.
- (35) Perrone, T. F.; Margerum, D. W. *Inorg. Chem.* To be submitted for publication.
- (36) Guha, S.; Francisco, J. S. *Chem. Phys. Lett.* Submitted for publication.

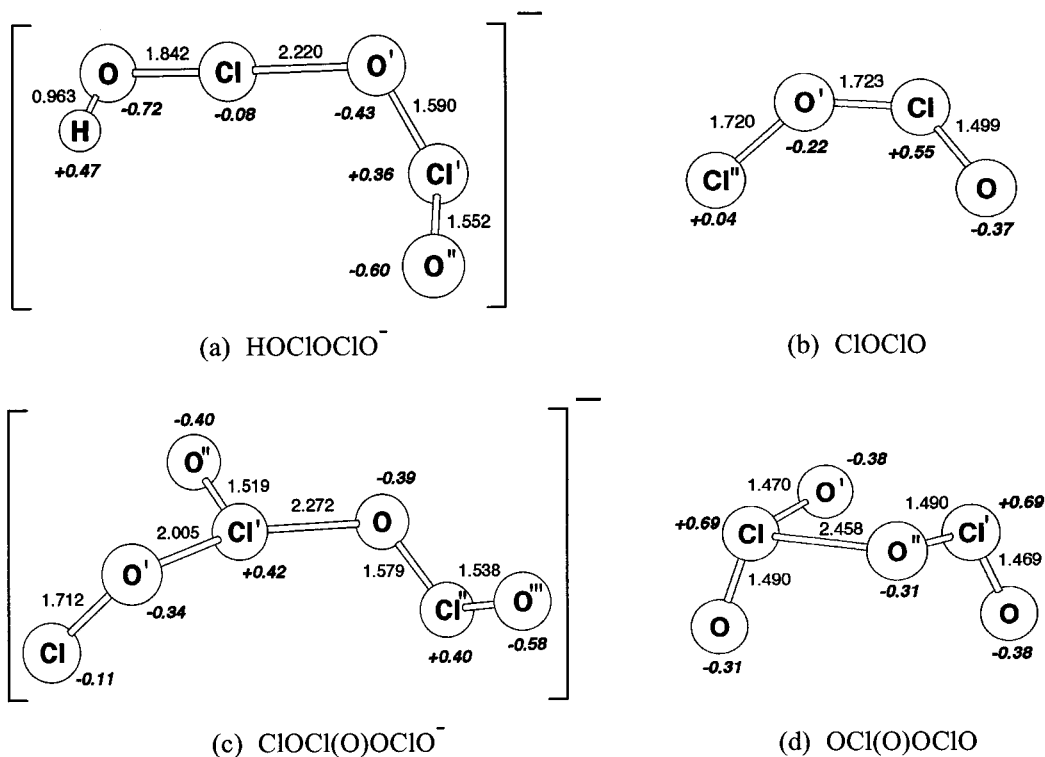


Figure 6. Equilibrium geometries (bond distances in angstroms) and atomic charges for key intermediates in the HOCl/ClO_2^- reactions.

ClO_2^- change by $+0.014$ and -0.024 Å when the HOCI(O)ClO^- (Figure 6a) adduct forms. Similar changes are found for the formation of HOBrOClO^- , where the O-Br (1.844 Å) bond length in HOBr increases by 0.139 Å to form the adduct. These rearrangements will contribute significantly to the activation barriers in the formation of the adducts.

Acknowledgment. This work was supported by National Science Foundation Grant CHE-98-18214. We thank the Jet Propulsion Laboratory at the California Institute of Technology for providing generous support of supercomputer time. The Cray

Supercomputer was provided by funding from the NASA Mission to Planet Earth, Aeronautics, and Space Science Program.

Supporting Information Available: Tables of kinetic data, equilibrium geometries, atomic charges, zero-point energies, and relative energies and figures showing a Brønsted–Pedersen plot and a relative energy diagram. This material is available free of charge via the Internet at <http://pubs.acs.org>.

IC991486R